The Space Congress® Proceedings | 1966 (3rd) The Challenge of Space

Mar 7th, 8:00 AM

Navigation for Spin Stabilized Deep Space Planetary Spacecraft

R. A. Park
TRW Systems

D. H. Newell
TRW Systems

Follow this and additional works at: https://commons.erau.edu/space-congress-proceedings

Scholarly Commons Citation

Park, R. A. and Newell, D. H., "Navigation for Spin Stabilized Deep Space Planetary Spacecraft" (1966). *The Space Congress® Proceedings*. 1.
https://commons.erau.edu/space-congress-proceedings/proceedings-1966-3rd/session-13/1

This Event is brought to you for free and open access by the Conferences at Scholarly Commons. It has been accepted for inclusion in The Space Congress® Proceedings by an authorized administrator of Scholarly Commons. For more information, please contact commons@erau.edu.

EMBRY-RIDDLE Aeronautical University
SCHOLARLY COMMONS

NAVIGATION FOR SPIN STABILIZED DEEP SPACE PLANETARY SPACECRAFT

R. A. Park
D. H. Newell
TRW SYSTEMS
California

Navigation for planetary missions is well understood as shown by the successful flights to Venus and Mars by the JPL Mariner spacecraft. However, when we consider the farther planets, such as Jupiter and ultimately Pluto, the trip time requirements are so long (on the order of 2 years to Jupiter and 8 to 10 years to Pluto) that spacecraft reliability becomes the paramount consideration.

A basic approach to achieving reliability is to simplify the spacecraft system as much as possible within the limits of mission objectives, which usually arise from the scientific payload. System simplicity and reliability can be greatly enhanced if the spacecraft system is spin stabilized, since this reduces control system requirements substantially and in general minimizes onboard navigation tasks.

However, spin stabilization itself imposes a number of problems which must be solved before such a simplifying technique can be adapted. As an illustration, the present Pioneer VI spacecraft is spin stabilized and has no onboard control requirements after the first few days of the mission; hence its lifetime appears to be limited only by the lifetime of the electronic components. Pioneer VI, shown in Figure 1, is injected in a heliocentric orbit while spinning and is then torqued by a nitrogen system to place its spin axis perpendicular to the plane of the ecliptic. A phased array antenna mounted along the spin axis then provides a fan beam pattern lying in the plane of the ecliptic, thus always illuminating the earth and assuring the constant communication with the DSIF for ranges up to 2 AU. All perturbing factors, such as solar pressure, have been accounted for and this spacecraft will apparently retain its attitude indefinitely. (There is a small change in body attitude during the course of 1/2 of the orbit around the sun but this change is cancelled out in the next 1/2 of the orbit).

The Pioneer VI spacecraft in its present configuration is not suitable for deep space missions beyond 2 AU from the sun because it uses solar cells for a power source. But if SNAP radioisotope thermo-electric generators (RTG) were used, this spacecraft could perform a fairly deep space mission limited only by the antenna gain. The gain of the fan beam antenna is restricted by the factor that the transmitted power is radiated over 360°, although in a fairly narrow beam ($\pm 2.5^{\circ}$). But this beam can be easily narrowed to 12° simply by using a reflector, as shown in Figure 2, with the antenna and increasing effective transmitted power by more than a factor of 10 and thus increasing communication range by more than a factor of 3.16.

The antenna reflector focusing the beam must be counter spun so that the beam points are always in the direction of the earth. Such a technique which has been investigated by TRW Systems, is basically simple and can be programmed as a function of position in the trajectory using either the sun or earth angle as an optical reference. A similar technique was used successfully on the Ball Brothers "OSO" earth satellite and operated for more than three years.

In this way even such a simple spacecraft as Pioneer VI could be used for a mission beyond the orbit of Jupiter. A picture of such a hypothetical spacecraft is shown in Figure 3. However the Pioneer VI spacecraft has no capability for mid-course guidance and hence is not suitable for planetary missions which require more accuracy than any booster vehicle alone can provide. Such a mid-course guidance system could be added to the Pioneer spacecraft quite simply and used to guide the Pioneer VI to any planet, providing that a suitable guidance method is available. TRW Systems has been interested in such a guidance technique since its first Pioneer I spacecraft which was launched toward the moon in 1958.

The method proposed is to mount a thrustor unit parallel with the spin axis and then find times during the course of the transfer orbit when firing this thrustor either backward or forward along the fixed spin axis reduces the injection errors so that the spacecraft will fly-by the planet with the required accuracy. Of course, this technique has a velocity penalty associated with it when compared to critical plane type maneuvers, but it may, nevertheless, increase the probability of mission success.

In addition to the Pioneer VI type of spin stabilized configuration, other configurations are possible. One which maximizes communications capability would clearly be desireable. Such a configuration is shown in Figure 4. As can be seen, this configuration is essentially a flying parabolic antenna. If this antenna is constantly pointing toward the earth, the bit rate at Jupiter's orbit is about 1,000 bits per second using only a 10 watt transmitter in the spacecraft. However, this configuration, while

very simple, has one more requirement than the Pioneer VI spacecraft; that is the body attitude must be kept pointing toward the earth which means that a torquing system must be used throughout the mission. In the beginning of the mission the spacecraft attitude must be moved about 1° a day, but as the spacecraft gets further and further from the earth the amount of motion required decreases steadily. Finally, when the spacecraft is at Jupiter's orbit, the body attitude will need to be moved only $\pm 9^{\circ}$ per year. The amount of cold nitrogen required for torquing such a spacecraft for a three year mission is less than 10 pounds. The ideal reference system for providing an error signal for the body attitude is the transmitted signal from the earth and a conical scan technique exploiting the spacecraft spin can be quite simply implemented. No moving sensors are required and the spacecraft attitude is immune to any perturbation other than a catastrophic impact from a micro-meteroid. This latter feature is of considerable importance since a ground transmission capability of the 2200 mc DSIF using its 210' antenna and a 100 KW transmitter is limited to about 5 AU when transmitting to an omni-directional antenna on the spacecraft. Thus, if it is necessary for the spacecraft body attitude to be changed and a reacquisition maneuver required, command capability at long ranges to the spacecraft during this maneuver would not be possible. The spin stabilized attitude suggested here insures the possibility of command communication to the spacecraft under all but catastrophic failure. There are other configurations, such as one with its spin axis always pointing toward the sun. Each has special characteristics, but in all configurations guidance must be possible.

We must now determine if it is in fact possible to make all of the required corrections with an arbitrary body attitude. Before entering a detailed description of the problems of this technique, let us illustrate how such a method works. What we do first is to examine the launch window for trajectories which make this technique effective. Figure 5 shows the launch window to Jupiter in 1968 as a function of trip time versus launch date for contours of constant injection energy. (Only trajectories which go less than 180° - Type I - are shown). For purposes of examination an arbitrary launch date of November 30 was selected with a trip time of 760 days. This date was selected largely because it was close to minimum energy for this launch window.

Figure 6 shows the effect of injection errors from a typical three stage launch vehicle upon arrival at the planet Jupiter. The assumed errors were 20 meters per second (1σ) in velocity and an angular error of 0.5° (1σ). While these errors are large, they are typical of a solid propellant third stage controlled only by spin during its thrusting period. The relative effects on the target miss caused from errors in the position vector at injection are small by comparison.

As can be seen, the semi-major axis of the uncorrected miss ellipse is 3.3 million kilometers (3σ) and the semi-minor axis is 1.5 million kilometers (3σ) for this trajectory.

An integrating computer program was used to fly the spacecraft to Jupiter on that date and mid-course sensitivities were computed for 10 specific days during transit; at injection and on the 1st, 2nd, 4th, 8th, 16th, 32nd, 64th, 128th, and 256th days. These sensitivities are plotted in Figure 7 for a spin stabilized spacecraft pointing always toward the earth. As can be seen, if we could make a correction immediately following injection we would be able to correct out 28,000 kilometers of miss per meter per second approximately in the negative B. R. direction, corresponding essentially to the semi-minor axis of our miss. Thus, if our dispersion was exactly at the maximum point of the semi-minor axis, we would require only 40 meters per second of propellant to correct total miss. In fact, of course, a specific mid-course guidance policy is established considering such factors as the mid-course sensitivity characteristics as a function of time, the number of expected correction maneuvers, the length of time required from injection and between maneuvers to ensure adequate tracking, the accuracy of the spin direction, the accuracy attainable in performing the correction maneuvers, the allowable target error dispersion, and the actual target error. Thus the first correction maneuver cannot be performed earlier than 4 to 8 days from injection. If two corrections can be made, for example at 4 and 175 days from injection, no more than 160 meters per second 3σ is required to remove an arbitrary target miss.

An illustration of the two correction maneuver scheme is presented in Figure 8. Because the mid-course correction sensitivities are generally not perpendicular to each other, the effects of two corrections at different times form a non-orthogonal basis in $B \cdot T$, $B \cdot R$ space. The dotted lines in the figure indicate how an arbitrary target error is removed. The letters A and B in the figure denote the correction maneuver sensitivities for two different times.

Since as we can see in Figure 7 the sensitivities do not rotate more than 120°, and since our error could be in any quadrant around the target point, the spacecraft must have the capability of thrusting in opposite directions to be sure that all errors can be satisfied. However, if the spacecraft has only one engine, the injection conditions could be biased off of the target, insuring that the single direction of thrust could reduce all components of error. However in general, this would result in a correction velocity penalty of about a factor of 2 greater than that required for a spacecraft with two motors and of course in terms of spacecraft weight is not desireable. Of course it is possible to thrust in the optimum direction that is in the critical plane. A curve of the required 3σ velocity loading as a function of time is computed and is shown in Figure 9. As can be seen from this curve, the minimum velocity requirement is at about 125 days after injection, which allows us an enormous amount of tracking time to determine our initial error. It should be pointed out that the characteristics shown in Figure 9 result from an out-of-plane effect which minimizes one component of correction corresponding in this case largely to a time of flight error which we do not attempt to correct. As is shown in Figure 10, the component which we do not have to correct for a fly by mission represents the greatest miss sensitivity coefficient.

Of course a single critical plane correction at the optimum time would minimize total propellant requirements, but it would be necessary to change the body attitude to an arbitrary direction which is not allowed under our ground rules. With the two correction scheme, the second correction will be required also to correct errors incurred during our first correction. The complete mission analysis will then require an iteration of the method that we have already described, using a second miss ellipse developed from an analysis of the errors incurred during the first mid-course correction. There will be of course always resuidal errors, but estimates, using DSIF tracking accuracy and available midcourse propulsion system accuracies, indicate that the two correction technique should reduce the injection error by at least a factor of 100, giving us miss at Jupiter of less than a Jupiter radius.

As is obvious in the description, to insure that all components of miss are corrected, it is critical that the miss sensitivities rotate as they did in fact rotate for the launch date selected here. Unfortunately this rotation does not always occur, and as will be shown later, for certain trajectories the sensitivities are essentially collinear and thus all components of miss can not be corrected with any body attitude. Figure 11 shows a 600 day flight time to Jupiter in 1971 in which the sensitivities are essentially collinear as a function of time, even though the spin axis remains Earth-pointing and therefore rotates in inertial space. Thus, first correction execution errors cannot be removed. Of course, even with an optimum critical plane correction a second midcourse might be required to eliminate first correction execution errors.

A detailed analysis of a spin stabilized mission to Venus has been performed for the 1968-69 launch window in order to gain insight into the mid-course guidance characteristics. This analysis is generally applicable to all planetary missions and the analytic approach appears also to apply to all other planets.

The spin axis attitudes selected for detailed study are characteristic of a Pioneer type spacecraft. The Pioneer is spin stabilized at injection into the interplanetary orbit. Two separate orientation maneuvers position the spin axis normal to the ecliptic. The first maneuver turns the spacecraft so that the spin axis is perpendicular to the sun line. This turn is controlled by sun sensors located about the equator of spin. Thus, the resulting spin axis may be mathematically represented by

$$\overline{S_1} = \frac{\left(\overline{R_s} \times \overline{S_o}\right) \times \overline{R_s}}{\left|\left(\overline{R_s} \times \overline{S_o}\right) \times \overline{R_s}\right|}$$

where $\overline{S_1}$ is the spin axis attitude after the turn, $\overline{R_s}$ is the spacecraft - sun vector, and $\overline{S_o}$ is the spin axis attitude at injection. The geometry is illustrated in Figure12. Because this orientation assures that the solar cell array intercepts the maximum amount of solar flux, this orientation may be maintained for a long period of time.

The second maneuver turns the spacecraft to place the spin axis approximately perpendicular to the ecliptic plane assuring that the high gain radio antenna sensitive direction may be oriented toward earth while maximum solar flux can still be intercepted by the solar cell array. The resulting spin axis direction $\overline{S_2}$, may be mathematically represented by

$$\overline{S}_2 = \frac{\overline{R}_s \times \overline{R}_e}{\left| \overline{R}_s \times \overline{R}_e \right|}$$

where $\overline{R}_e$ is the spacecraft - earth direction. The geometry is illustrated in Figure 13.

Mid-course correction motors may be located in several effective positions on a spin stabilized spacecraft. The most convenient location which enables spacecraft stability to be maintained during motor firing is at the ends of the spacecraft along the spin axis. Thus, velocity may be imparted to the spacecraft along the spin axis in two opposite directions. For this study, it is assumed that the two motors are mounted in this manner.

The trajectories selected for this study include 13 trajectories representative of the complete launch window for the 1968-69 launch opportunity to Venus. Certain parameters are tabulated in Table I identifying the characteristics of these trajectories. In addition, the selected trajectories are identified in Figure 14, a plot of flight time versus launch date for several injection energies.

Figure 14 has two separate groups of energy contours, denoted as Type I and Type II trajectories. Type I trajectories are defined as having heliocentric transfer angles less than 180°, and Type II trajectories are those having heliocentric transfer angles greater than 180°. For a given launch day, Type I trajectories have shorter flight times than do Type II trajectories. The boundary between the Type I and II contours is a single point; for this launch day, flight time and energy, the spacecraft leaves Earth and arrives at Venus at either the ascending or descending node of Venus' orbit.

For each of the two trajectory types, the trajectories are further divided into two classes, denoted Class I and Class II. Class I trajectories are identified by the broken contours in Figure 14. For a given launch day, energy, and trajectory type, Class I trajectories have shorter flight times than do Class II trajectories.

In addition, Table I includes the heliocentric central angle, and a qualitative indication how close the trajectory is to a minimum energy trajectory for that launch day. These parameters will be considered in a later section.

To indicate the sensitivities of injection errors upon deviations from the desired target point in a way consistent for all 13 trajectories, the trajectory dependent $\overline{R}$-$\overline{S}$-$\overline{T}$ Venus centered coordinate system is used. This coordinate system is illustrated in Figure 15. $\overline{S}$ is a unit vector collinear with the incoming hyperbolic approach asymptote passing through the center of Venus; $\overline{T}$ is normal to $\overline{S}$ lying in a plane parallel to the ecliptic plane including Venus; and $\overline{R}$ completes the righthanded system. Because $\overline{S}$ depends upon each trajectory characteristic near Venus, the coordinate systems will differ in inertial space for each trajectory. A parameter $\overline{B}$, called the impact parameter, is measured in this coordinate system to denote the miss from the target. In this study, the distance of closest approach to the planet is of concern and the time of closest approach is unimportant. Thus, two quantities, $\overline{B}\cdot\overline{T}$ and $\overline{B}\cdot\overline{R}$ indicate the deviation of the approach asymptote from direct passage through the center of Venus in the two coordinate directions $\overline{T}$ and $\overline{R}$. This geometry is illustrated in Figure 16.

Errors in the injection velocity vector $\left[\Delta\dot{x}_i \quad \Delta\dot{y}_i \quad \Delta\dot{z}_i\right]^T$ are linearly related to errors in the nominal miss $\overline{B}\cdot\overline{T}$ and $\overline{B}\cdot\overline{R}$. Thus, (dropping the bar notation)

$$\begin{bmatrix} \Delta B\cdot T \\ \Delta B\cdot R \end{bmatrix} = \begin{bmatrix} \frac{\partial(B\cdot T)}{\partial\dot{x}_i} & \frac{\partial(B\cdot T)}{\partial\dot{y}_i} & \frac{\partial(B\cdot T)}{\partial\dot{z}_i} \\ \frac{\partial(B\cdot R)}{\partial\dot{x}_i} & \frac{\partial(B\cdot R)}{\partial\dot{y}_i} & \frac{\partial(B\cdot R)}{\partial\dot{z}_i} \end{bmatrix} \begin{bmatrix} \Delta\dot{x}_i \\ \Delta\dot{y}_i \\ \Delta\dot{z}_i \end{bmatrix}$$

or

$$\Delta M = C\Delta V_i$$

It will be assumed for this study that errors in the position vector at injection have negligible effect. In the matrix C, the 2 x 1 column vectors, called miss coefficient vectors, indicate in B·T and B·R coordinate space the magnitude and direction of a unit error in each of the injection velocity vector components.

The velocity injection errors are statistically represented by a covariance matrix Σ_I defined by

$$\Sigma_I = E\left[\Delta V_i \, \Delta V_i^T\right]$$

where the E indicates expected value. Because injection errors are linearly related to the components of miss at the target, the uncorrected miss at the target caused from these injection errors are statistically represented as

$$\Sigma_T = C \Sigma_I C^T$$

To make the mid-course guidance investigation as independent as possible of launch vehicle types, the injection covariance matrix Σ_I will be assumed diagonal with equal elements. Thus

$$\Sigma_I = kI$$

and

$$\Sigma_T = \begin{bmatrix} \sigma_{11} & \sigma_{12} \\ \sigma_{21} & \sigma_{22} \end{bmatrix} = k\, CC^T$$

where k is a scalar quantity equal to the variance in any xyz direction, and I is a 3 x 3 unit matrix. Such an approximation compares with covariance matrices computed for actual launch vehicles. An exception is that the correlated terms in an actual covariance matrix are non zero which can cause the resulting target covariance matrix to differ somewhat depending upon the characteristics of the miss coefficient vectors.

Consideration of the various factors inherent to a complete midcourse guidance policy results in difficult analyses to determine the mid-course velocity requirements. A-priori selection of the variables allows an analysis to be performed and the midcourse velocity requirements computed, but the complexity of such an analysis precludes a parametric study for a great many trajectories to be performed, for example, to minimize the midcourse velocity requirements. Instead a reasonable estimate of the mid-course velocity requirements will be made based on the general characteristics of the injection errors and the correction sensitivities of the trajectories considered.

Several quantitative characteristics for each of the trajectories have been computed and are plotted in Figures 17 through 30. Included in each figure are the sensitivities of the velocity injection errors plotted in B·T, B·R space for a 1 meter per second perturbation in each of the injection velocity components; the size of Σ_T, indicated by the eigen values of this matrix which represent the semi-major and semi-minor axes of the 1σ miss ellipse normalized for k = 1 meter per second squared; and the effects of a 1 meter per second velocity increment added in the same sense along the spacecraft spin axis as the injection velocity increment for the three spin attitudes S_0, S_1, and S_2 as a function of time. Thus, for one mid-course correction motor mounted collinear with the spin axis, only target errors in B·T, B·R space located along an imaginary extension of the mid-course sensitive direction shown in the plots in the diagonal quadrant can be removed with one motor firing. For two motors mounted at each end of the spin axis, target errors located anywhere along the imaginary extension of the sensitive lines can be removed with one motor firing.

The mid-course correction sensitivities can be categorized into three general groups. The first group, denoted group A, are typified by the characteristics of trajectory numbers 1, 4, 6, and 7. The sensitivities, nearly constant in direction, are only weakly influenced by time or spin axis orientation. These trajectories have miss ellipses with large major to minor axis ratios; for trajectory number 6, the miss ellipse is a thin silver. Because of the collinear characteristics of the sensitivities, not all arbitrary target errors can be eliminated even if an arbitrary spin direction can be assumed (such as required for a critical plane correction). Therefore, the trajectories of this group are unacceptable for our spin stabilized guidance scheme.

The second group, called B, includes trajectory numbers 2, 3, 8, and 9. The correction sensitivity directions in this group are influenced more strongly by spin axis orientation but, like group A, are only weakly influenced by time. This group has miss ellipses more circular than group A. Because of the spin axis dependency of the sensitivities, arbitrary target errors can be removed.

The third group, called C, includes trajectory numbers 5, 10, 11, 12, and 13. The correction sensitivity directions of these trajectories exhibit the strongest effect of time and spin axis orientation. The miss ellipses are moderately eccentric - more like the ellipses of group A. The rotation of the sensitivities enables arbitrary target errors to be removed.

A characteristic common to all groups is the reduction of the correction sensitivity magnitudes as a function of time during a major portion of each flight.

The characteristics of the correction sensitivities of group B appear more favorable than those of group C for a multiple attitude spacecraft like Pioneer because of the relative orthogonality of the sensitivities for each spin orientation. The sensitivities of group C rotate to cause relative orthogonality, but in order to gain advantage of this phenomena, require that the first correction be performed very soon after launch. Such a requirement does not

allow for adequate tracking prior to the first correction, but delay of the maneuver would increase the mid-course guidance propulsion requirements. However the characteristics of group C are essential for spacecraft with an inertially - fixed spin axis.

The guidance equation which relates the velocity increments for each of n correction maneuvers to the target errors is

$$\begin{bmatrix} \Delta B \cdot T \\ \Delta B \cdot R \end{bmatrix} = -D \begin{bmatrix} \Delta V_1 \\ \Delta V_2 \\ \vdots \\ \Delta V_j \\ \vdots \\ \Delta V_n \end{bmatrix}$$

or

$$\Delta M = -D\Delta V$$

where ΔV_j are the magnitudes of the correction manuevers at different times,

$$D = \left[C'_1 \mid C'_2 \mid \cdots \mid C'_j \mid \cdots \mid C'_n \right]$$

and C'_j are the mid-course correction sensitivity matrices for a certain spin orientation and time. For three or more corrections, a unique combination of velocity increments does not exist. For two corrections however

$$\Delta V = -D^{-1} \Delta M$$

The velocity requirements for two corrections are statistically represented by a covariance matrix $\Sigma_{\Delta V}$ defined by

$$\Sigma_{\Delta V} = D^{-1} \Sigma_T D^{-1^T}$$

3σ estimates of the total velocity requirements are obtained by multiplying the square root of the trace of $\Sigma_{\Delta V}$ by 3.

Mid-course correction velocity requirements were computed for a Pioneer type spacecraft for trajectory number 2, typical of group B, considering the normalized injection covariance matrix and several values of k.

Two correction maneuvers were selected, the first 6 days from launch in the $\overline{S}_1$ attitude, and the second 20 days from launch in $\overline{S}_2$ attitude. In addition, the covariance matrix

$$\underset{\sim}{\Sigma}_I = \begin{bmatrix} .04 & 0 & 0 \\ 0 & 1 & 0 \\ \rho & 0 & 1 \end{bmatrix} 10^{-2} \text{ km/sec}$$

was considered, which corresponds to velocity injection errors of 20 meters/sec, 0.01 rad, and 0.01 rad in polar coordinates. No errors in the correction maneuvers were assumed.

At the time of this writing, our study was not complete and the trajectory physics are not entirely explicable. However, certain of the mid-course correction sensitivity characteristics can be explained by examining the geometry of the trajectories and the injection energies. Trajectory numbers 1, 4, and 6 of group A, for example, have heliocentric transfer angles near 180^0, which causes velocity components added near injection and perpendicular to the plane of the trajectory to be ineffective in changing the trajectory path in the vicinity of the target. This phenomena can be observed for these trajectories by noting how the injection error sensitivities are collinear but with different magnitudes. The correction sensitivities remain aligned in this manner for various spin attitudes and times. The time independence is not fully understood.

The trajectories of group C are characterized by requiring near minimum injection energy and a non-180^0 transfer angle. These all have considerable rotation of the sensitivities. Trajectories which require minimum energy exhibit a particular characteristic. Consider a polar coordinate form of the injection velocity vector:

$$\overline{V}_i = \begin{bmatrix} V_i \\ \beta_i \\ A_i \end{bmatrix}$$

where β_i is flight path angle and A_i is azimuth at injection. There is one family of solutions V_i, β_i, and A_i which cause the spacecraft to intercept the target planet. Different points of this family correspond to different flight times. If V_{io}, β_{io}, and A_{io} is one solution of the family, then a point at $V_{io} + dV_i$, $\beta_{io} + d\beta_i$, and $A_{io} + dA_i$ will be a solution if

$$\begin{bmatrix} \frac{\partial(B\cdot T)}{\partial V_i} & \frac{\partial(B\cdot T)}{\partial \beta_i} & \frac{\partial(B\cdot T)}{\partial A_i} \\ \frac{\partial(B\cdot R)}{\partial V_i} & \frac{\partial(B\cdot R)}{\partial \beta_i} & \frac{\partial(B\cdot R)}{\partial A_i} \end{bmatrix} \begin{bmatrix} dV_i \\ d\beta_i \\ dA_i \end{bmatrix} = 0$$

If injection occurs exactly at minimum energy, then

$$\frac{\partial V_i}{\partial \beta_i} = \frac{\partial V_i}{\partial A_i} = 0$$

and therefore

$$\frac{\partial V_i}{\partial \beta_i} d\beta_i + \frac{\partial V_i}{\partial A_i} dA_i = dV_i = 0$$

and the equations above reduce to

$$\begin{bmatrix} \frac{\partial(B\cdot T)}{\partial \beta_i} & \frac{\partial(B\cdot T)}{\partial A_i} \\ \frac{\partial(B\cdot R)}{\partial \beta_i} & \frac{\partial(B\cdot R)}{\partial A_i} \end{bmatrix} \begin{bmatrix} d\beta_i \\ dA_i \end{bmatrix} = 0$$

One row (or column) of the 2 x 2 matrix is proportional to the other. This means that the angular injection error sensitivities are parallel in $B\cdot T$, $B\cdot R$ space and different from the V_i error sensitivity. For times different from t_i injection, these angular error sensitivities move with respect to each other causing rotation of the mid-course maneuver sensitivities for a given attitude. Higher energy trajectories as shown by group B vary not with time, but with body attitude.

While we do not have as yet a complete analytical solution to our problem, additional analyses of the correction sensitivities for various body attitudes are currently in progress.

The authors are indebted to A. B. Mickelwait, T. A. Magness, J. B. McGuire, R. A. Tompkins, P. Lavoie and R. Bobrow of TRW Systems for their invaluable help. We also thank Ruby Williams for her editorial assistance.

References:

Clarke, V. C.; Bollman, W. E.; Roth, R. Y; Scholey, W. J., Design Parameters for Ballistic Interplanetary Trajectories, Part I One-Way Transfers to Mars and Venus. Jet Propulsion Laboratory TR No. 32-77 January 16, 1963.

Table 1. Trajectory Characteristics

Trajectory Number	Launch Date	Flight Time (Days)	Trajectory Type	Trajectory Class	Injection Energy ($m^2/sec^2 \times 10^8$)	Near Minimum Energy? *	Central Angle (Deg)
1	12-10-68	146	I	I	.160	Yes	161
2	1-14-69	100	I	I	.170	No	108
3	2-4-69	84	I	I	.170	No	96
4	1-8-69	136	I	II	.090	No	163
5	1-14-69	126	I	-	.077	Yes	152
6	11-16-68	178	II	I	.170	Yes	200
7	1-19-69	194	II	II	.170	No	260
8	3-15-69	184	II	II	.210	No	279
9	3-8-69	154	II	I	.170	No	227
10	1-19-69	178	II	-	.132	Yes	234
11	1-27-69	176	II	-	.130	Yes	237
12	2-8-69	170	II	-	.130	Yes	248
13	1-27-69	112	I	-	.092	Yes	137

* For the specified launch day.

Table 2. Midcourse Correction Velocity Requirements for Trajectory 2

Injection Covariance Matrix	Velocity Requirements (3-σ)
Normalized with $k = (10 \frac{m}{s})^2$	15.5 $\frac{m}{s}$
Normalized with $k = (100 \frac{m}{s})^2$	155 $\frac{m}{s}$
$\hat{\Sigma}_I$	122 $\frac{m}{s}$

First correction maneuver at 6 days in $\bar{S}_1$ attitude.
Second correction maneuver at 20 days in $\bar{S}_2$ attitude.
Figure 30 shows the miss ellipse for Σ_I

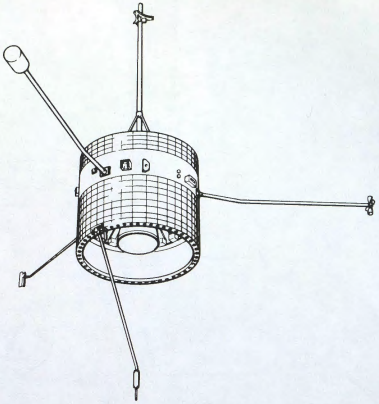

Figure 1. Spin-Stabilized Spacecraft – Perpendicular to the Elliptic Pioneer VI

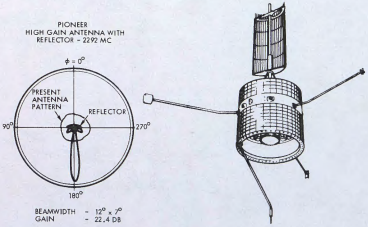

Figure 2. Pioneer VI with Antenna Reflector

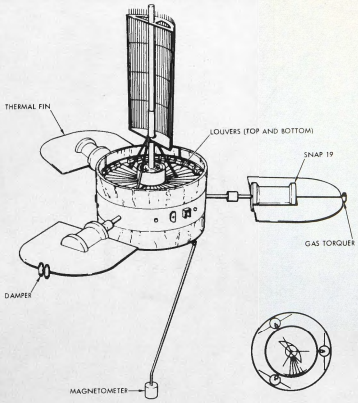

Figure 3. Pioneer VI with Radioisotope Thermoelectric Generators and Despin Reflector

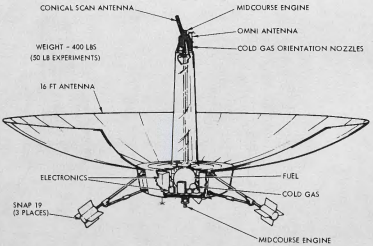

Figure 4. Earth-Pointing Spin-Stabilized Spacecraft

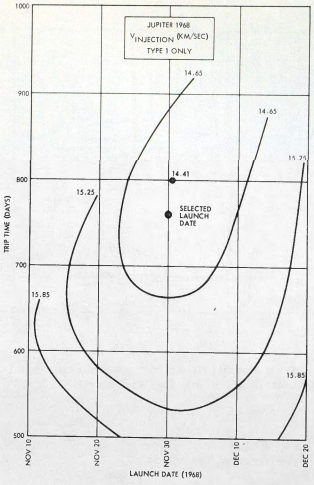

Figure 5. Launch Window Characteristics for Jupiter 1968

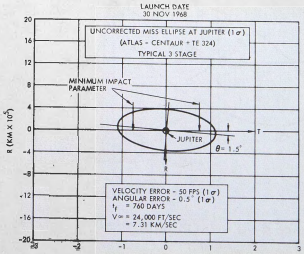

Figure 6. Uncorrected Miss Ellipse at Jupiter (Solid Propellant Spin-Stabilized 3rd Stage)

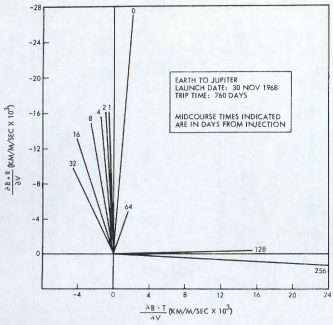

Figure 7. Midcourse Sensitivities for a Spin-Stabilized Spacecraft Continuously Pointing Toward Earth

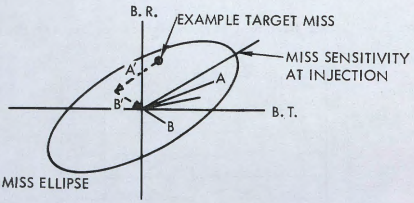

Figure 8. Two Correction Maneuver Scheme

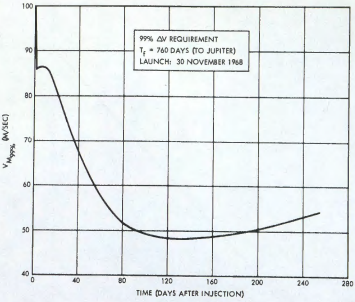

Figure 9. ΔV Requirement for a Critical Plane Correction (Jupiter 1968)

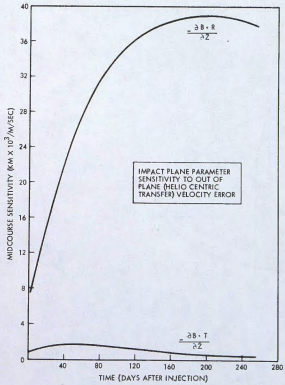

Figure 10. Components of Midcourse Sensitivity for a 30 November 1968 Launch; 760 Flight Time

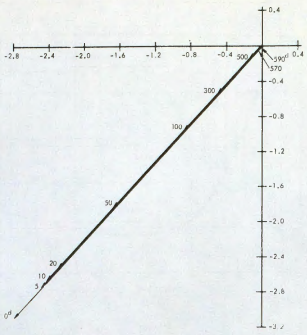

Figure 11. Midcourse Sensitivities of a Spin-Stabilized Spacecraft Always Pointing Toward Earth (1971 Launch)

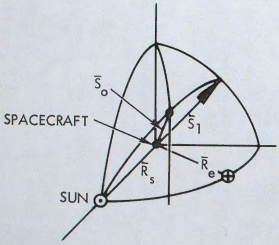

Figure 12. $\bar{S}_1$ Attitude Geometry

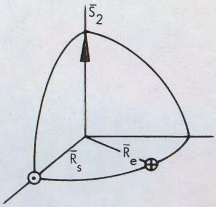

Figure 13. $\bar{S}_2$ Attitude Geometry

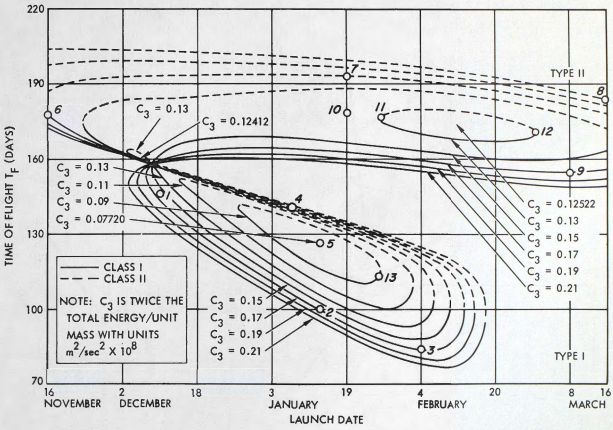

Figure 14. Venus Launch Window (1968-69)

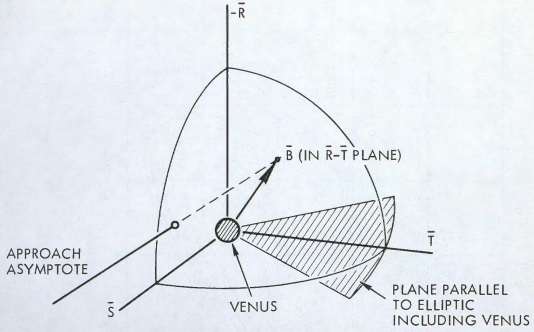

Figure 15. $\bar{R}$-$\bar{S}$-$\bar{T}$ Coordinate Definition

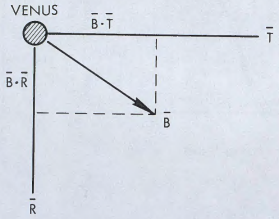

Figure 16. $\bar{B} \cdot \bar{T}$ and $\bar{B} \cdot \bar{R}$ Definition

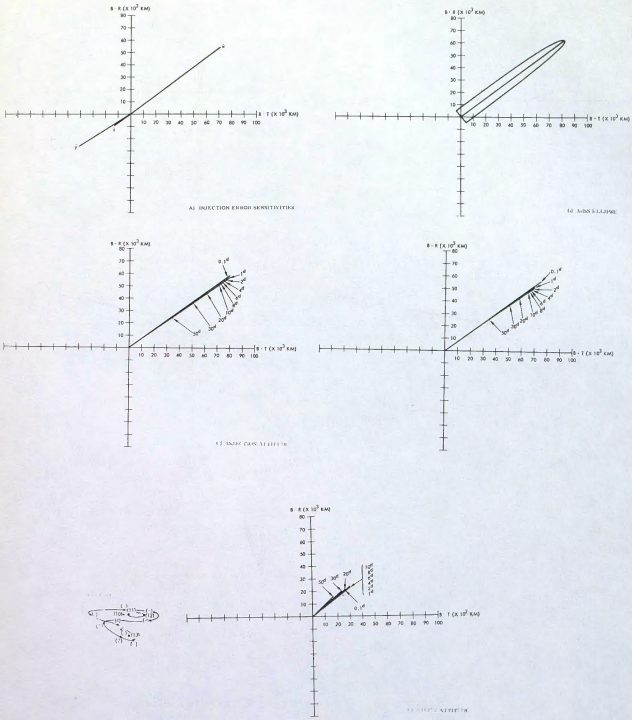

Figure 17. Trajectory 1 Characteristics

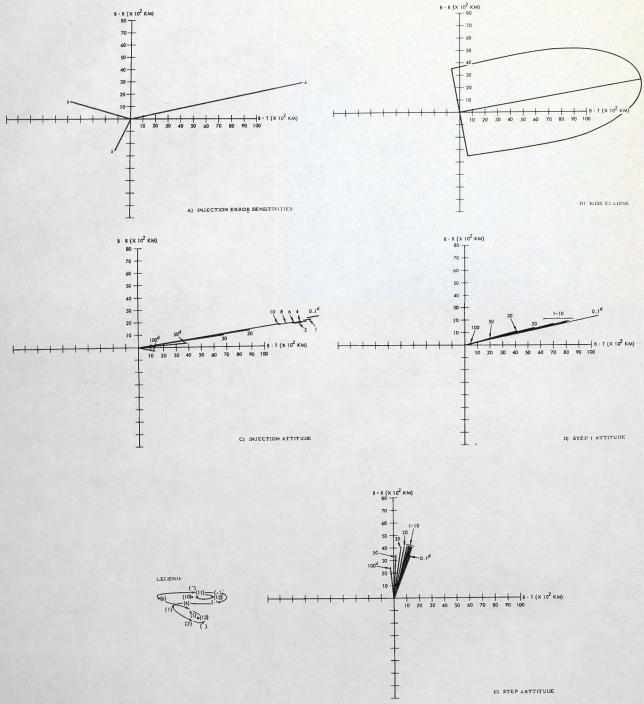

Figure 18. Trajectory 2 Characteristics

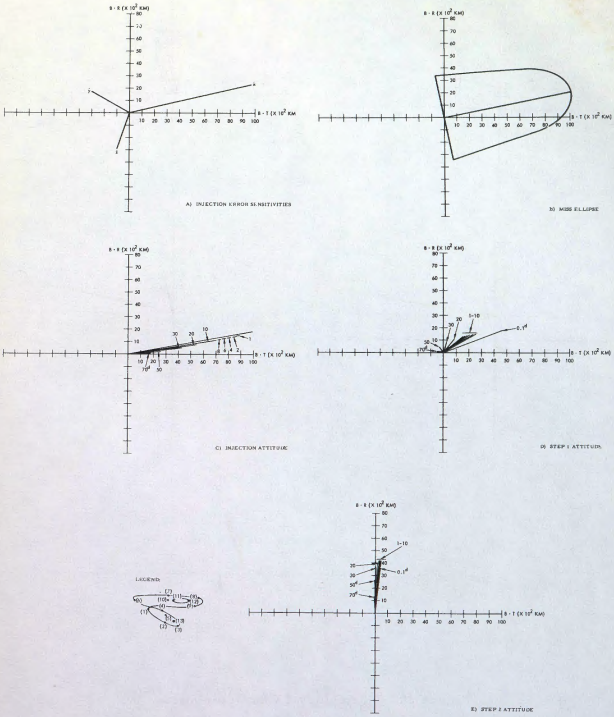

Figure 19. Trajectory 3 Characteristics

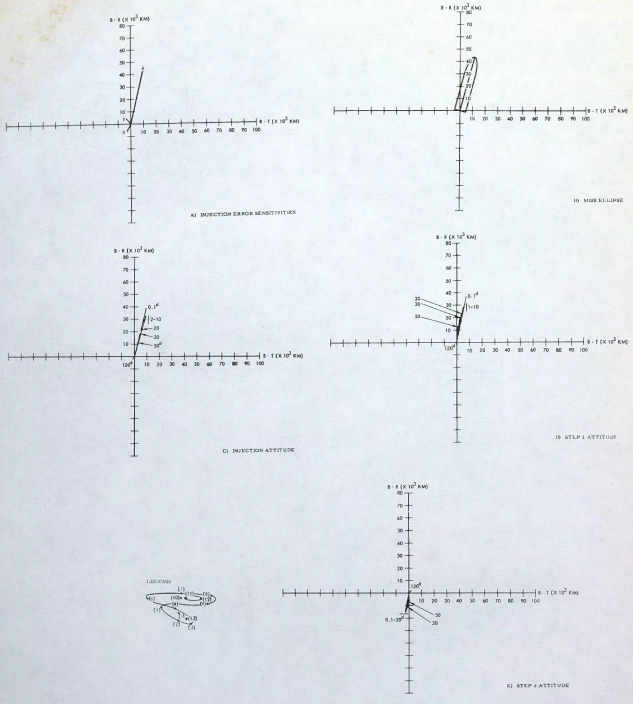

Figure 20. Trajectory 4 Characteristics

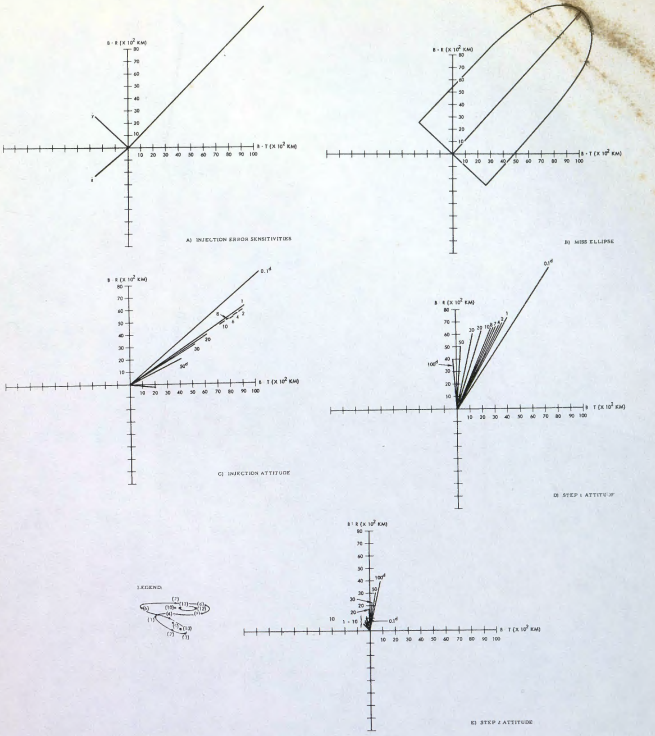

Figure 21. Trajectory 5 Characteristics

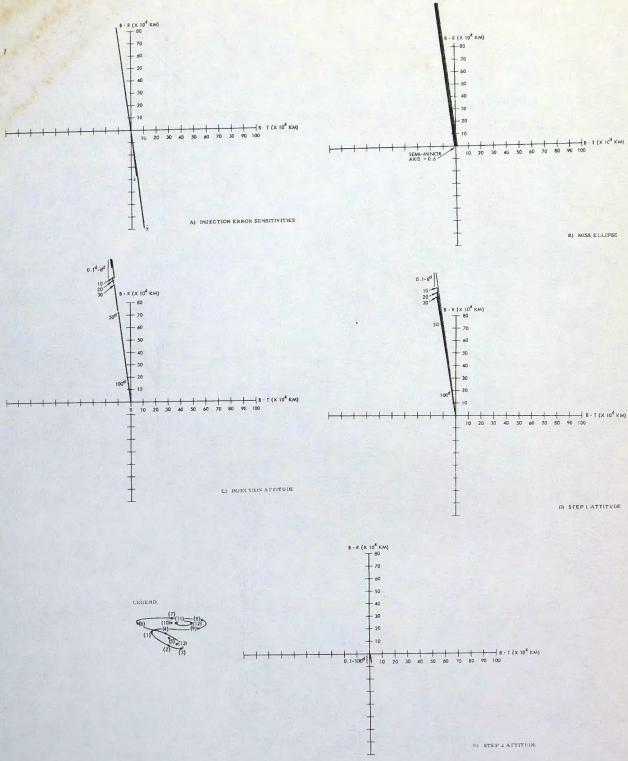

Figure 22. Trajectory 6 Characteristics

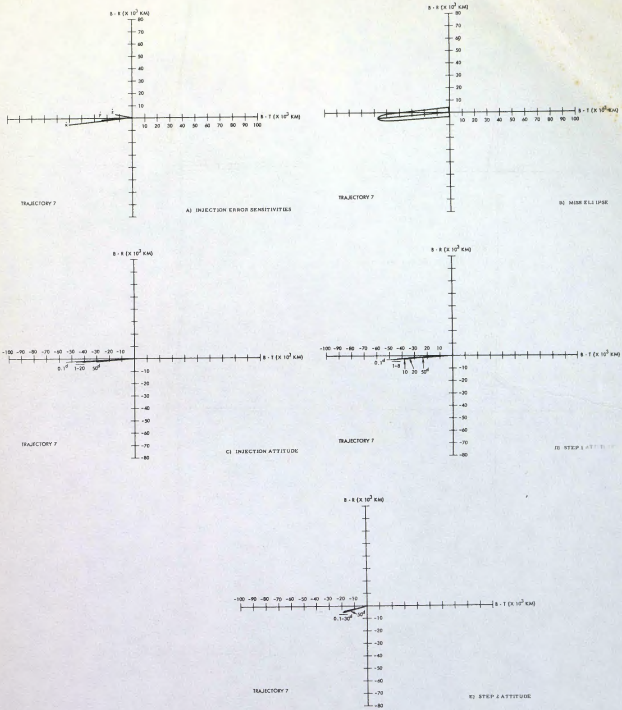

Figure 23. Trajectory 7 Characteristics

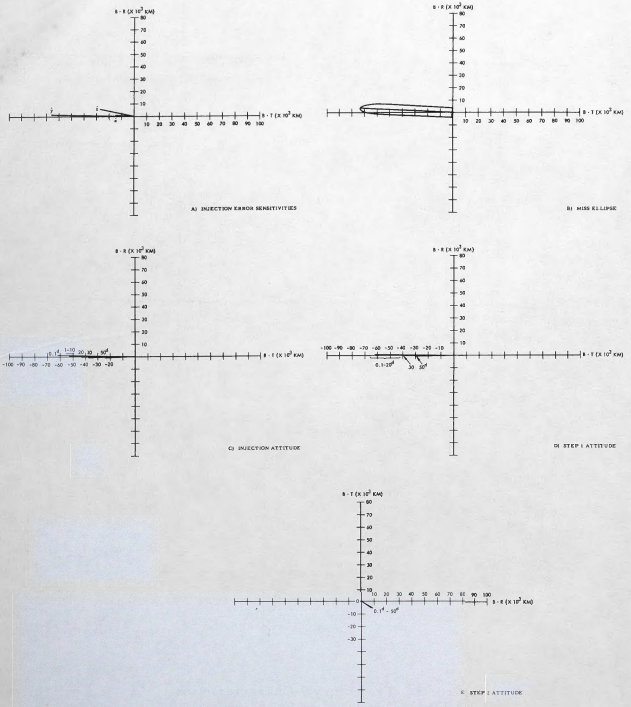

Figure 24. Trajectory 8 Characteristics

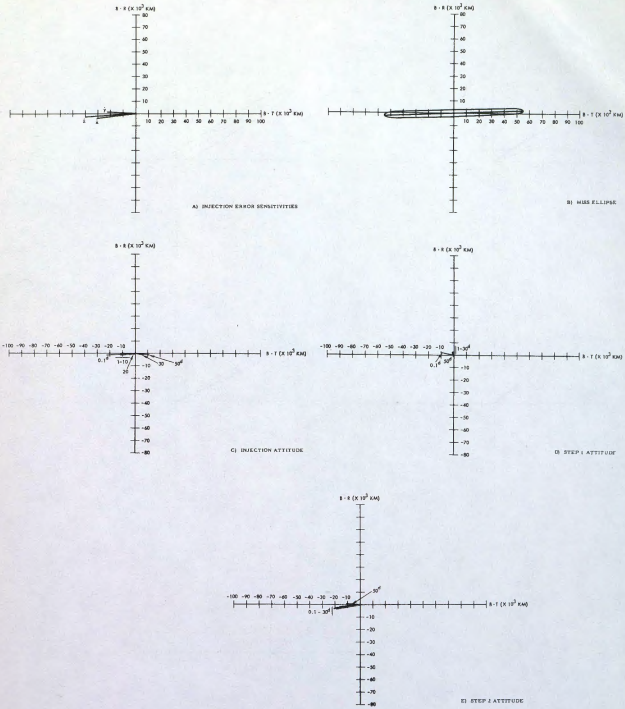

Figure 25. Trajectory 9 Characteristics

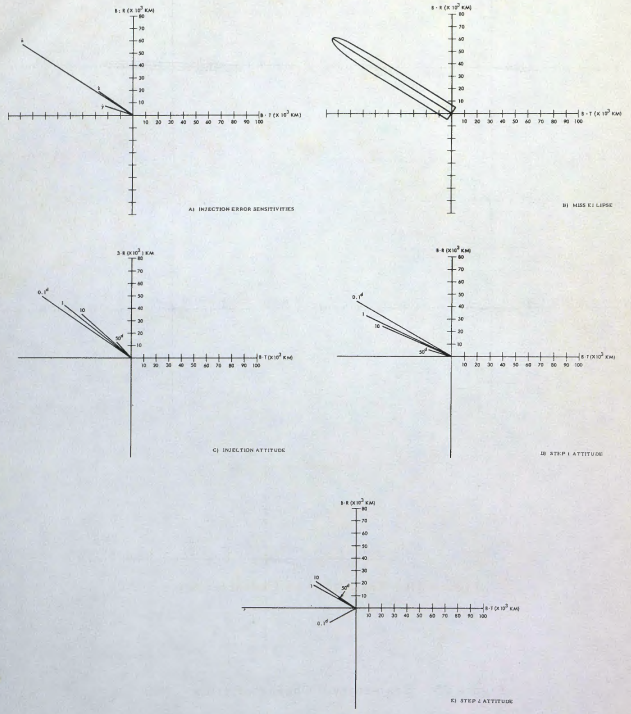

Figure 26. Trajectory 10 Characteristics

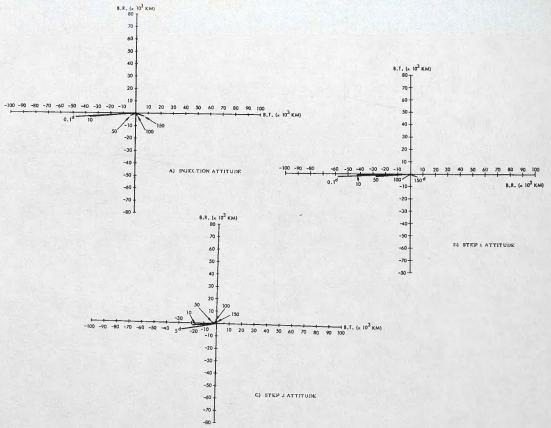

Figure 27. Trajectory 11 Characteristics

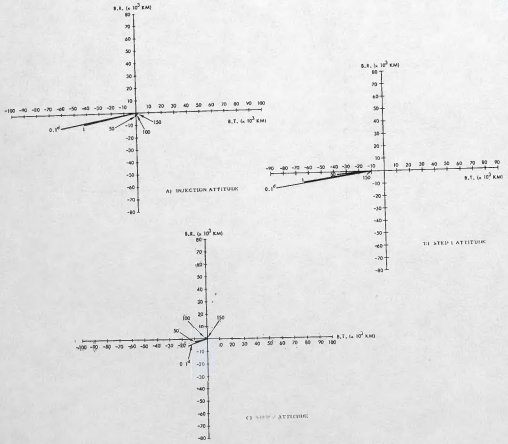

Figure 28. Trajectory 12 Characteristics

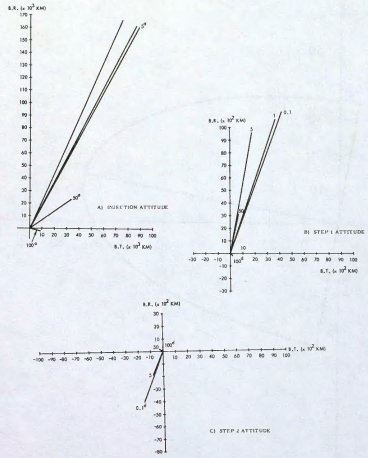

Figure 29. Trajectory 13 Characteristics

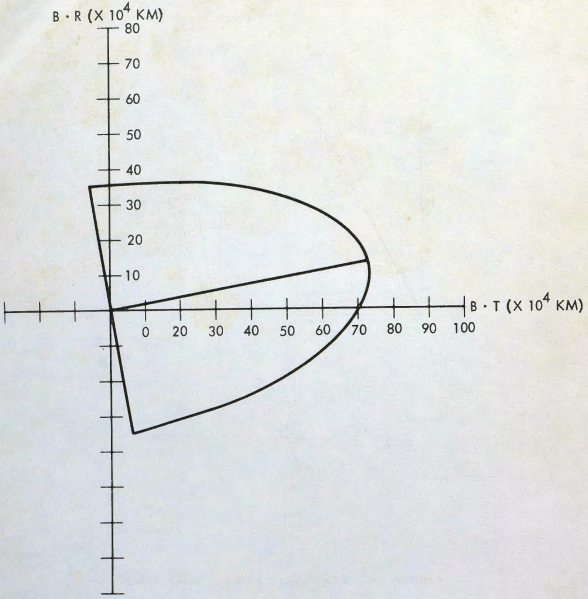

Figure 30. Uncorrected Miss Ellipse for Trajectory 2 (Injection Errors = 60 m/sec and 0.03 rad) (3σ)